

1 Jet sub-structure and parton shower evolution in 2 p+p and Au+Au collisions at STAR

Raghav Kunnawalkam Elayavalli for the STAR Collaboration*

Wayne State University, Detroit MI 48201

E-mail: raghavke@wayne.edu

Recent measurements of jet structure modifications at RHIC and LHC highlight the importance of differential measurements to study the nature of jet quenching. Since these jet structure observables are intimately dependent on parton evolution in both the angular and energy scales, measurements are needed to disentangle these two scales in order to probe the medium at different length scales to study its characteristic properties such as the coherence length. To that effect, the STAR collaboration presents fully unfolded results of jet sub-structure observables designed to extract fundamental quantities related to the parton shower via the SoftDrop shared momentum fraction (z_g), the groomed jet radius (R_g) and the jet Mass (M) in p+p collisions at $\sqrt{s} = 200$ GeV as a function of jet transverse momenta. Having established the p+p baseline, we present the first measurement of the jet's inherent angular structure in Au+Au collisions at $\sqrt{s_{NN}} = 200$ GeV via an experimentally robust observable related to the SoftDrop R_g : the opening angle between the two leading sub-jets (θ_{SJ}). In Au+Au collisions at STAR, we utilize a specific di-jet selection as introduced in our previous momentum imbalance (A_J) measurement and measure both the A_J and the recoil jet spectra differentially as a function of the angular classes based on the θ_{SJ} observable. With such measurements, we probe the medium response to jets at a particular resolution scale and find no significant differences in quenching for jets of different angular scales as given by θ_{SJ} .

*13th International Workshop on High-pT Physics in the RHIC/LHC era
19 - 22 March 2019
Knoxville, Tennessee, USA*

*Speaker.

3 1. Introduction

4 Relativistic ion collisions produce copious amounts of jets due to the hard scatterings between
 5 quarks and gluons of the colliding nuclei. Recent measurements at both RHIC and LHC along with
 6 theoretical advancements have shown the importance of studying and measuring the properties of
 7 these jets both in p+p and in heavy ion collisions (reviews of jet studies can be found here [1]).
 8 There are two natural scales that characterize a jet and its evolution: the momentum and the angular
 9 scales. First generation jet measurements have measured jet quenching in an integrative manner,
 10 for example via the momentum asymmetry in di-jet events and have further extensively studied the
 11 momentum dependence via nuclear modification factors and fragmentation functions. Jet-medium
 12 interaction could further be dependent on the resolution scale or the coherence length of the medium
 13 which perceives the jet as a singular radiating object or a multi-prong object [2].

14 2. Jet sub-structure in p+p Collisions

15 In order to differentially study energy loss in the QGP medium, the jet structure in vacuum
 16 has to be first understood at both momentum and virtuality scales related to the DGLAP splitting
 17 functions [3] that govern parton evolution. In recent literature, SoftDrop [4] has gained fame as an
 18 algorithm which can extract such scales experimentally with its procedure of walking backwards
 19 in the Cambridge/Aachen clustering tree until two sub-jets satisfy $z = \frac{\min(p_{T,1}, p_{T,2})}{p_{T,1} + p_{T,2}} > z_{cut} (\Delta R/R)^\beta$
 20 where z_g and R_g are the z and ΔR upon termination of the algorithm with $z_{cut} = 0.1$ and $\beta = 0$.
 21 It was shown that for such choices of z_{cut}, β the SoftDrop z_g distribution converges to the vacuum
 22 DGLAP splitting functions for $z > z_{cut}$ in a ‘‘Sudakov-safe’’ manner [5]. The invariant jet mass is
 23 also measured as a function varying jet p_T since it is dependent on the virtuality scale set by the
 24 parton shower.

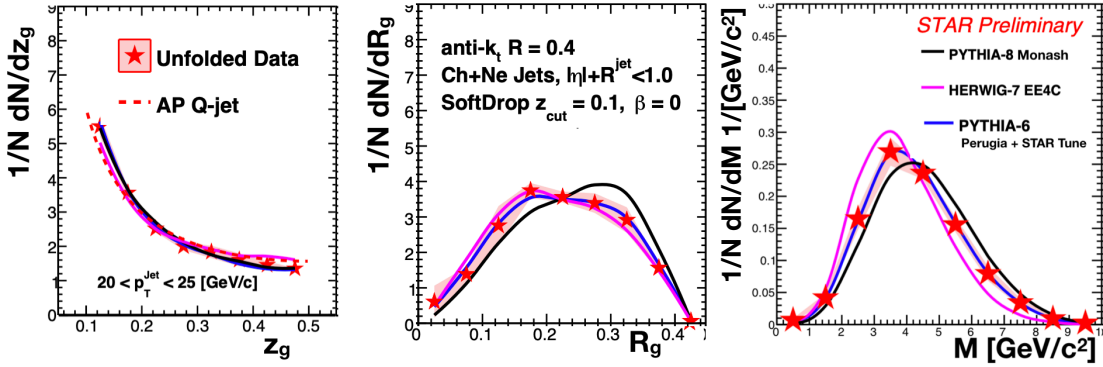


Figure 1: Fully unfolded measurement of the SoftDrop groomed sub-jet shared momentum fraction (z_g), the groomed jet radius (R_g) and the jet mass in p+p collisions at $\sqrt{s} = 200$ GeV for jets with $20 < p_T < 25$ GeV/c. The markers and lines are described in the text.

25 The p+p data for the jet sub-structure measurements were collected with the STAR detec-
 26 tor [6] during the 2012 run at $\sqrt{s_{NN}} = 200$ GeV. Jets are reconstructed from charged tracks in the
 27 Time Projection Chamber (TPC) and energy depositions in the Barrel ElectroMagnetic Calorimeter
 28 (BEMC) using the anti- k_t algorithm as implemented in the FastJet package [7], hereafter referenced

29 as Ch+Ne jets. For additional details regarding event/track/tower quality selections, please refer
 30 to [8, 9, 10]. Two-dimensional unfolding in p_T and z_g , R_g , M respectively, is done using Bayesian
 31 unfolding as implemented in the RooUnfold package [11, 12] with four iterations. The response
 32 matrix is created from a PYTHIA-6 (Perugia Tune, slightly adapted to STAR data) [14] prior and
 33 a GEANT-3 simulation of the STAR detector. The systematic uncertainties for data are taken as a
 34 quadrature sum resulting from the following sources: tracking efficiency (4%), tower gain calibra-
 35 tion (3.8%), hadronic correction to the tower energy scale (described in [8]) and unfolding-related
 36 sources including varying the iteration parameter from 2 to 6 and the prior in the response matrix.

37 Figure 1 shows the fully unfolded z_g (left), R_g (middle) and M (right) distributions for jets with
 38 $20 < p_T < 25$ GeV/c, respectively. The STAR data are shown in the red filled star markers with the
 39 red shaded region corresponding to the overall systematic uncertainty. Leading order Monte Carlo
 40 (MC) generators such as PYTHIA-6 Perugia tune, PYTHIA-8 Monash [15], and Herwig-7 EE4C
 41 UE tune [16] in the blue, black and magenta lines are also plotted for comparison to the data. For
 42 the z_g observable, we also provide the symmetrized DGLAP splitting functions (noted as AP Q-Jet
 43 in the figure) at leading order in the red dashed lines for quark jets (with the splitting being similar
 44 for quark- and gluon-initiated jets). All the models studied reproduce the general trends seen in
 45 the data, particularly the dependence on the jet momenta leading to a steeper z_g distribution and a
 46 narrower R_g . As the jet mass is related to both the momentum and angular scales, the differences
 47 we see in both z_g and R_g carry over onto the mass with PYTHIA-8 and HERWIG-7 predicting
 48 larger and smaller masses respectively.

49 3. Jet Angular Scale in Au+Au Collisions

50 The Au+Au data used in these proceedings were collected during the 2007 run with its corre-
 51 sponding reference p+p run in 2006 at $\sqrt{s_{NN}} = 200$ GeV. Since the jet patch trigger is saturated in
 52 an Au+Au event, we employ a high tower (HT) trigger, requiring at least one BEMC tower with E_T
 53 > 5.4 GeV. Event centrality in Au+Au is determined by the raw charged track multiplicity in the
 54 TPC within $|\eta| < 0.5$ and we show only events in the 0-20% centrality range. In Au+Au events,
 55 we have two separate jet collections given by the HardCore selection [8], where jets are clustered
 56 with objects (tracks/towers) with $p_T > 2$ GeV/c, and Matched jets which are clustered from the
 57 constituent-subtracted [17] event with our nominal $p_T > 0.2$ GeV/c for constituents, and are ge-
 58 ometrically matched to the HardCore jets ($\Delta R < 0.4$). Further event selection criteria include a
 59 minimum p_T requirement for HardCore di-jets ($p_T^{\text{Lead}} > 16$, $p_T^{\text{SubLead}} > 8$ GeV/c) and an azimuthal
 60 angle ($|\Delta\phi(\text{Lead}, \text{SubLead})| > 2\pi/3$) selection to focus on back-to-back di-jets.

61 In our studies, we found the groomed jet radii (R_g) to be highly sensitive to the fluctuating
 62 underlying event in Au+Au collisions and therefore we devised a new observable involving sub-
 63 jets of a smaller radius reconstructed within the original jet (see here [13] for a recent theoretical
 64 article demonstrating similar classes of observables). For our nominal anti- k_t jets of $R = 0.4$, we
 65 reconstruct an inclusive set of anti- k_t sub-jets with $R = 0.1$ from the original jet's constituents. An
 66 absolute minimum sub-jet p_T requirement of 2.97 GeV/c is enforced in central Au+Au collisions
 67 to reduce sensitivity to the background fluctuations. The two observables related to the momentum
 68 and angular scales are then defined as follows $z_{SJ} = \frac{\min(p_T^{SJ1}, p_T^{SJ2})}{p_T^{SJ1} + p_T^{SJ2}}$, and $\theta_{SJ} = \Delta R(SJ1, SJ2)$, where
 69 $SJ1, SJ2$ are the leading and sub-leading sub-jets, respectively.

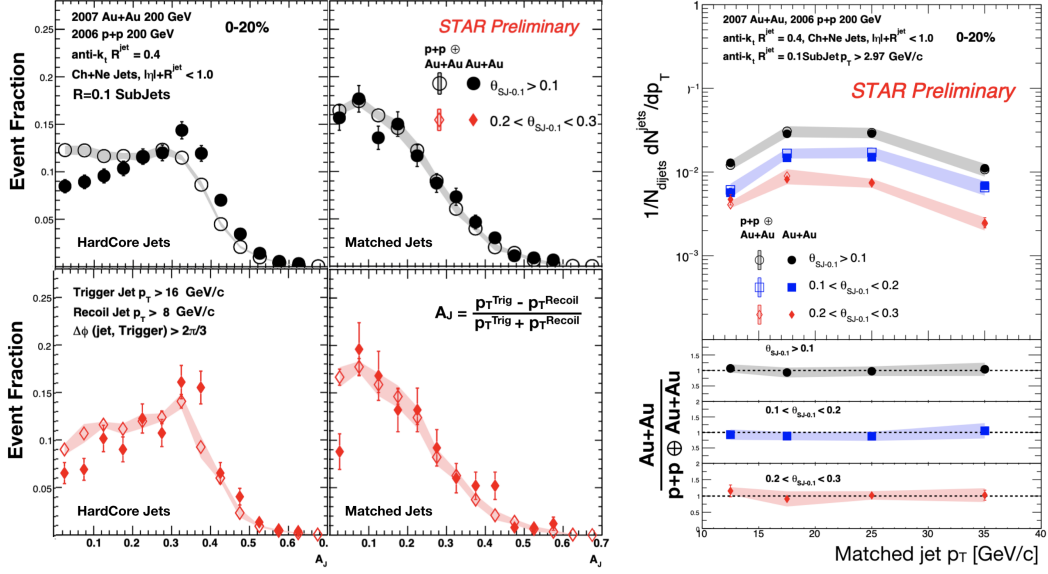


Figure 2: HardCore and Matched (left figure) di-jet asymmetry ($|A_J|$) and the Matched recoil jet yield (right figure) along with the ratios shown in the bottom right panels. Markers are described in the text.

70 For a meaningful comparison between Au+Au and a p+p reference, the effects of background
 71 fluctuations and detector inefficiencies must be taken into account. To achieve this, HT-triggered
 72 p+p data from 2006 is embedded into minimum bias Au+Au data (p+p⊕Au+Au) from 2007, in the
 73 same centrality range (0-20%). During embedding, we account for the relative tracking efficiency
 74 ($90\% \pm 7\%$) and relative tower energy scale ($100\% \pm 2\%$), with a one sigma variation taken as sys-
 75 tematic uncertainties. The TwoSubJet z_{SJ} and θ_{SJ} distributions for constituent-subtracted Matched
 76 recoil jets with $R = 0.1$ sub-jets (henceforth denoted as $SJ - 0.1$ in the figures) recoiling off the
 77 trigger (selected with $|\Delta\phi(\text{jet}, \text{HT})| > 2\pi/3$), in the p_T range 10-20 GeV/c are observed to be
 78 similar in both Au+Au and p+p⊕Au+Au [10]. We also observe a remarkable difference in the
 79 shape of z_{SJ} when compared to that of the SoftDrop z_g , which is caused by selecting the core of
 80 the jet. The θ_{SJ} for jets within the considered p_T range peaks at small values and includes a natural
 81 lower cutoff at the sub-jet radius and we now select jets based on this distribution.

82 Di-jet asymmetry for both HardCore and Matched jets (left panels) are shown in Fig. 2. The
 83 right panels of Fig. 2 show the yield of Matched recoil jets normalized per di-jet for the different
 84 θ_{SJ} selections and the ratios of Au+Au/p+p in the bottom panels. The black, blue and red markers
 85 represent recoil jets with selections on θ_{SJ} $[0.1, 0.4]$, $[0.1, 0.2]$ and $[0.2, 0.3]$ for inclusive, narrow
 86 and wide jets, respectively. We observe a clear di-jet imbalance indicating jet quenching effects in
 87 the $|A_J|$ distributions (comparing Au+Au to p+p⊕Au+Au) for all HardCore jets including the wide
 88 angle jets. The Matched jets on the other hand are balanced at RHIC energies, as evident by ratios
 89 in the bottom right panels consistent with unity. This is consistent with our earlier measurement [8].
 90 We also note that wide angle jets are still balanced indicating no apparent distinction between wide
 91 and narrow jets by the medium in our selection. Further detailed differential analyses are required
 92 with the high statistics 2014 data set to extract the medium resolution scale or the coherence length
 93 and the effect on standard jet quenching observables at RHIC energies.

94 4. Conclusions

95 STAR has presented the first fully unfolded jet substructure measurements including the Soft-
96 Drop z_g and R_g and jet Mass of inclusive jets with varying transverse momentum in p+p collisions
97 at $\sqrt{s}=200$ GeV. The measurements are overall reproduced by current leading order Monte Carlo
98 event generators for jets in our kinematic acceptance and reflect the momentum dependent narrow-
99 ing of jet structure. Due to the sensitivity of the SoftDrop observables to the Au+Au underlying
100 event, we introduce and measure the TwoSubJet observables, z_{SJ} and θ_{SJ} for $R=0.1$ anti- k_t sub-jets
101 as representing the momentum and angular scales of a jet in a heavy ion environment. We measure
102 the di-jet momentum asymmetry and the recoil jet yield with the special di-jet selection at STAR
103 and find that HardCore di-jets are imbalanced and Matched di-jets are balanced for jets of varying
104 angular scales. We find no significant difference in the quenching phenomenon for both wide and
105 narrow jets leading to the conclusion that these special jets do not undergo significantly different
106 jet-medium interactions due to their varying angular scales.

107 References

- 108 [1] M. Connors, R. Reed, S. Salur, C. Nattrass, Rev. Mod. Phys. 90, (2018) 025005
109 [2] Y. Mehtar Tani, K. Tywoniuk, Phys. Rev. D 98 (2018) 051501(R)
110 [3] G. Altarelli, G. Parisi, Nucl. Phys. B126 (1977) 298-318
111 [4] A. J. Larkoski, S. Marzani, G. Soyez, J. Thaler, JHEP 05 (2014) 146
112 [5] A. J. Larkoski, S. Marzani, J. Thaler, Phys. Rev. D 91 (11) (2015) 111501
113 [6] K. H. Ackermann et. al., Nucl. Instrum. Methods Phys. Res., Sect. A 499, (2003) 624
114 [7] M. Cacciari, G. P. Salam, G. Soyez, JHEP 04 (2008) 005.
115 [8] L. Adamczyk, et al., Phys. Rev. Lett. 119 (6) (2017) 062301
116 [9] Nick Elsey for the STAR Collaboration PoS HardProbes2018, 87 (2018)
117 [10] RKE for the STAR Collaboration, PoS HardProbes2018, 90 (2019)
118 [11] T. Adye et. al. hepunix.rl.ac.uk/~adye/software/unfold/RooUnfold.html
119 [12] G. D'Agostini, arXiv:1010.0632
120 [13] L. Apolinário, J. G. Milhano, M. Ploskon, X. Zhang, Eur. Phys. J. C78 (2018) no.6, 529
121 [14] T. Sjostrand, S. Mrenna, P. Z. Skands, JHEP 05 (2006) 026
122 [15] T. Sjostrand, et. al., Comput. Phys. Commun. 191 (2015) 159-177.
123 [16] M. Bahr, et al., Eur. Phys. J. C58 (2008) 639-707.
124 [17] P. Berta, M. Spousta, D. W. Miller, R. Leitner, JHEP. 1406 (2014) 092